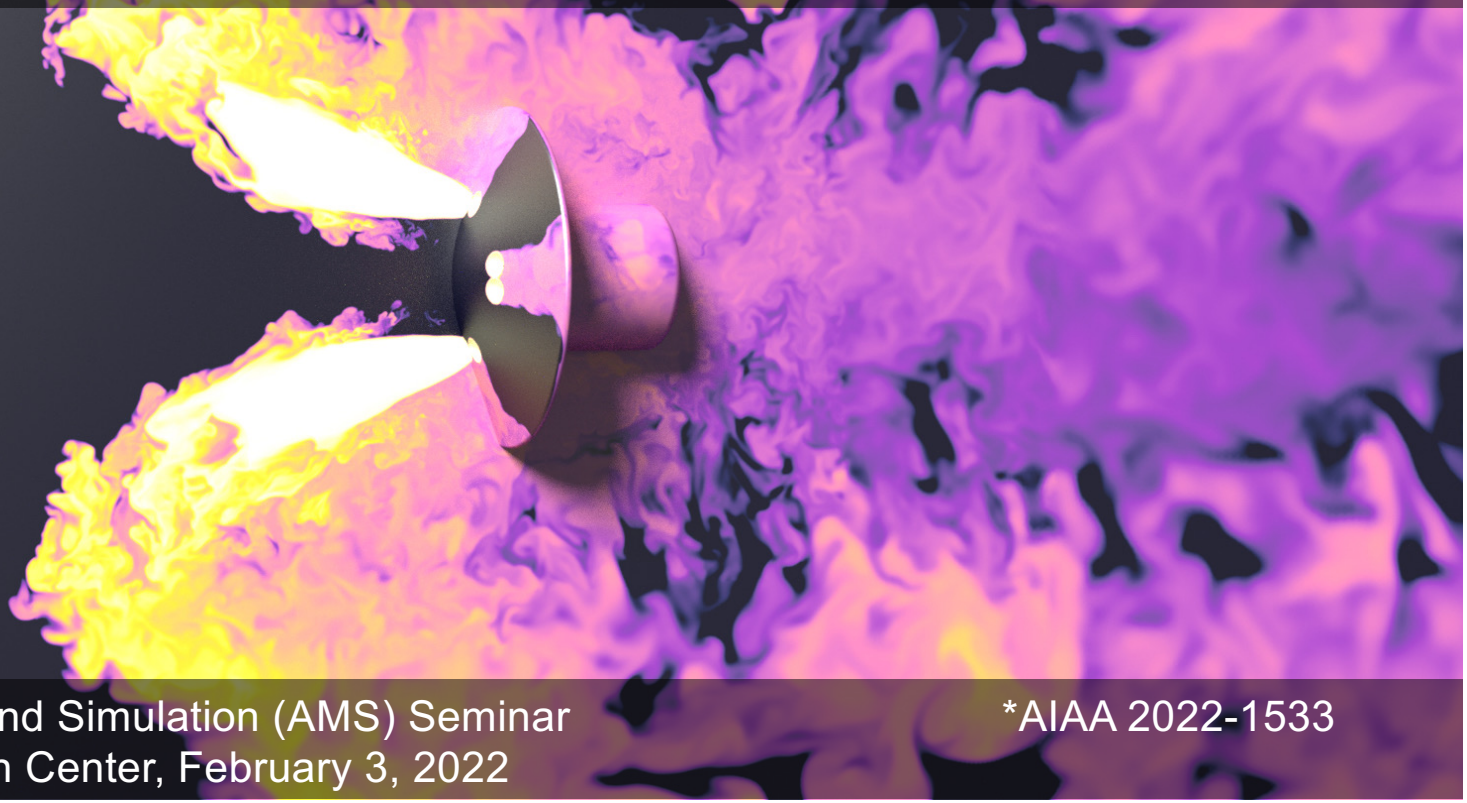
Scale-Resolving Simulations of a Supersonic Retro-Propulsion Concept For Mars Entry, Descent, and Landing*



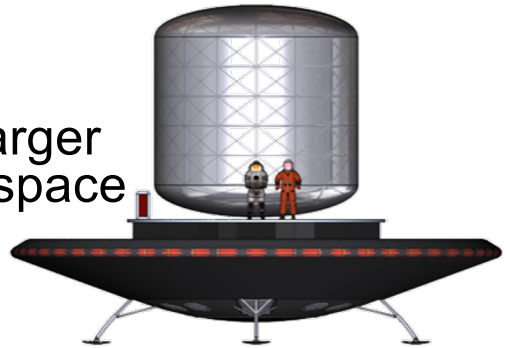
Francois Cadieux
Scott Neuhoff
Michael Barad
Cetin Kiris

Computational Aerosciences Branch
NASA Ames Research Center

Advanced Modeling and Simulation (AMS) Seminar
NASA Ames Research Center, February 3, 2022

*AIAA 2022-1533

Enabling Mars Human Exploration



What is Supersonic Retro-Propulsion (SRP)?

- SRP is a deceleration technology that could enable larger payloads and potentially humans to be brought from space to the surface of Mars safely

Why use SRP?

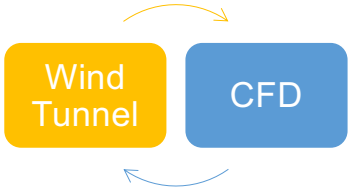
- Supersonic parachute and sky-crane maneuver used for Mars rovers so far can support a payload mass up to ~1-2 metric ton. Human exploration missions will require ~20 tons.

When/where to use SRP?

- Use blunt body drag to decelerate from atmospheric entry down to Mach 2.4 to 2.5, then turn on the SRP rockets to decelerate from Mach 2.4 to landing

Background

- Wind tunnel tests dating back to the beginning of the space race explored the physics of SRP and demonstrated the potential of this approach for Entry, Descent and Landing (EDL)
- Recent and planned wind tunnel entries focus on providing benchmark data for the validation of CFD to ground predictions



- CFD and wind tunnel experiments each have different strengths and weaknesses
- Need to strategically leverage both to gain confidence in our ability to design a reliable Mars EDL vehicle that uses SRP

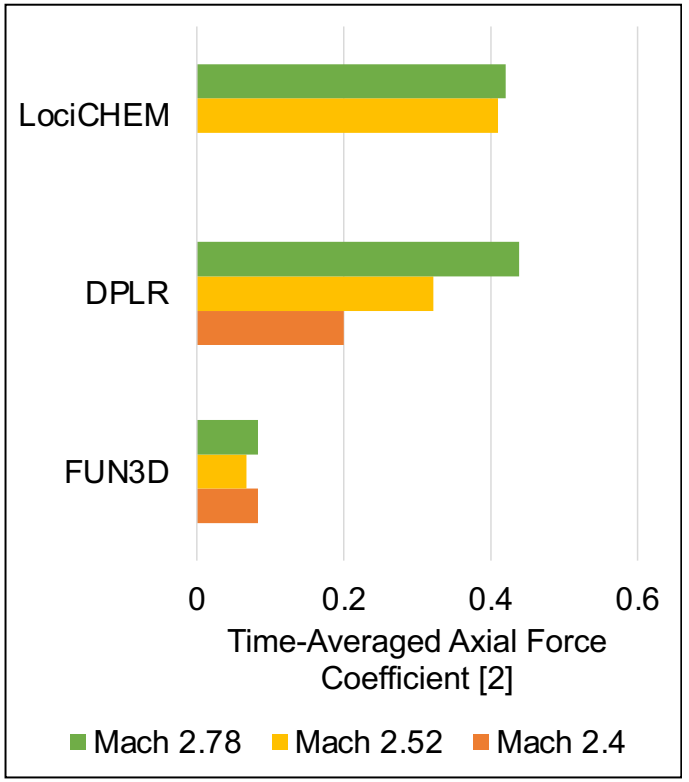


Sample Schlieren result for quad-nozzle at Mach 4.6, $\alpha = 0$, $\beta = 0$, and CT = 0.91 [1]

[1] Codoni, Joshua, and Scott Berry. "Analysis of Dynamic Data from Supersonic Retropropulsion Experiments in NASA Langley's Unitary Plan Wind Tunnel." *42nd AIAA Fluid Dynamics Conference and Exhibit*. 2012.

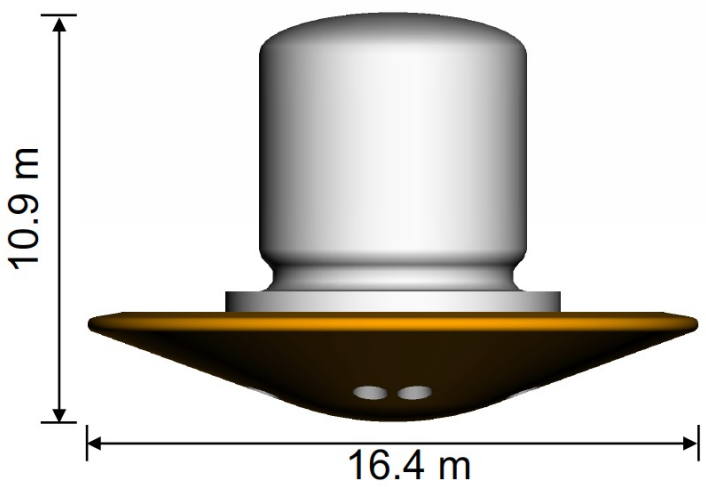
Motivation for CFD of SRP

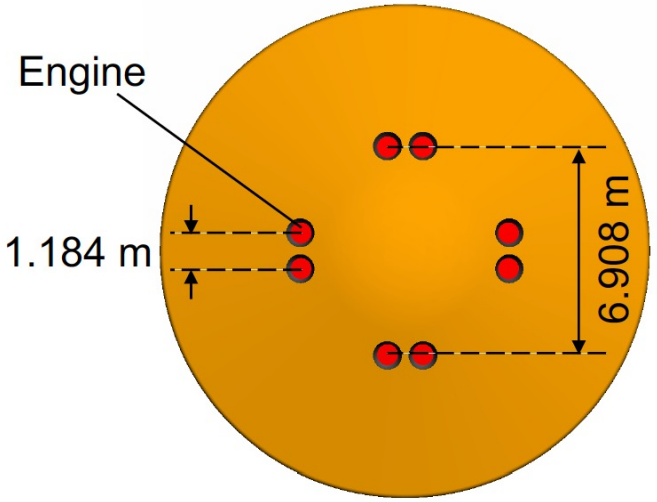
- Develop best practices so that CFD can be relied upon to design future Mars EDL system
- Multi-year collaborative efforts across NASA yielded significant progress toward validating steady Euler CFD predictions as well as steady and unsteady Reynolds-Averaged Navier-Stokes (RANS) CFD predictions with benchmark wind tunnel experiments for under-expanded SRP rocket plume regime
- Recent RANS results [2] show disagreements for full-scale flight vehicle powered simulations in the over-expanded plume regime spanning the altitudes and Mach numbers (2.4 to 2.78) associated with points in the trajectory where SRP could be first initiated for low L/D concept Mars EDL vehicle



[2] Korzun, A. M., Tang, C., Rizk, Y., Canabal, F., Childs, R., Van Norman, J. W., Tynis, J. A., and Bibb, K., "Powered Descent Aerodynamics for Low and Mid Lift-to-Drag Human Mars Entry, Descent and Landing Vehicles," AIAA Scitech 2020 Forum

Target SRP Vehicle For Mars EDL





- Conceptual full-scale low lift-over-drag (L/D) vehicle for Mars Entry, Descent & Landing (EDL)
- Hypersonic Inflatable Aerodynamic Decelerator (HIAD) heatshield with rigid connector and surface habitat payload
- 8 liquid oxygen-methane motors each capable of producing 100kN thrust (177:1 A/A^*), but throttled to 80% thrust

Overarching Goals



- Simulate full-scale vehicle in Mars atmosphere (97% CO_2, 3% N_2) at high altitude where the motors might first be initiated corresponding to the challenging over-expanded plume regime ($\frac{p_e}{p_\infty} \geq 1$)

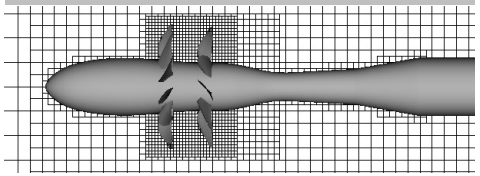
Case	M_∞	V_∞ (m/s)	T_∞ (K)	p_∞ (Pa)	q_∞ (Pa)	ρ_∞ (kg/m^3)
1	2.52	587.63	216.19	273.37	1155.67	0.0067
2	2.40	560.60	216.53	284.73	1093.82	0.0070
6	2.78	642.78	214.95	235.35	1212.83	0.0058

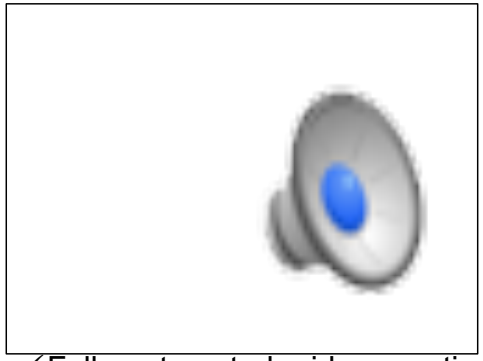
- Investigate grid convergence and provide grid-related uncertainty for vehicle drag prediction (axial force coefficient C_A excluding rocket thrust)
- Determine whether such simulations can be performed on current NASA High-End Computing Capability (HECC) resources in a short-enough turnaround time to affect engineering design decisions

CFD Grid Paradigms in LAVA



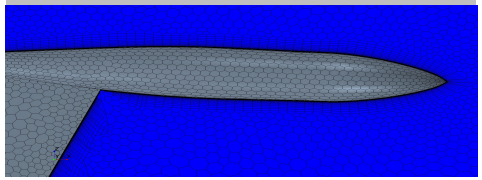
Structured Cartesian AMR

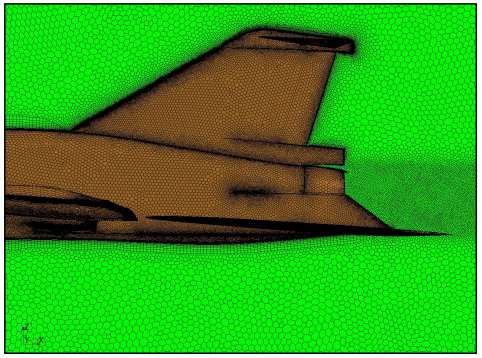




- ✓ Fully-automated grid generation
- ✓ Highly efficient Adaptive Mesh Refinement (AMR)
- ✓ Low computational cost
- ✓ Reliable higher order methods
- ✗ Non-body fitted → Resolution of boundary layers challenging

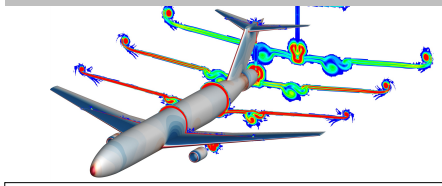
Unstructured Arbitrary Polyhedral

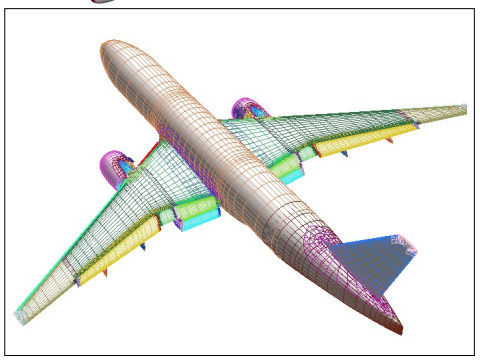




- ✓ Partially automated grid generation
- ✓ Body fitted grids
- ✗ Grid quality can be challenging
- ✗ High computational cost
- ✗ Higher order methods yet to fully mature

Structured Curvilinear





- ✓ High quality body fitted grids
- ✓ Low computational cost
- ✓ Reliable higher order methods
- ✗ Grid generation largely manual and time consuming

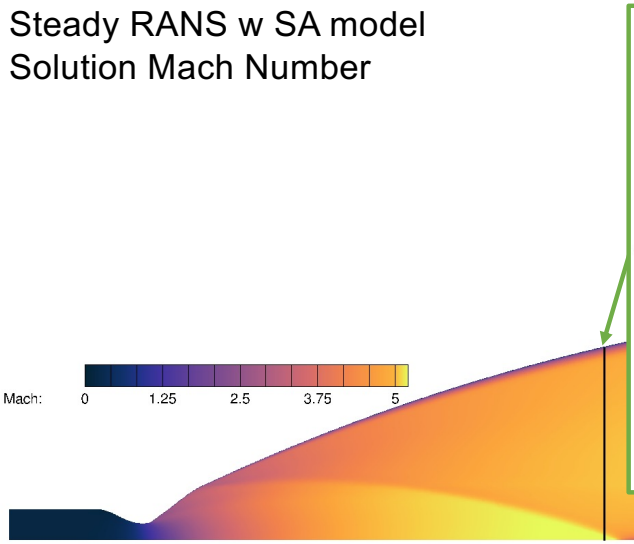
Simulation Strategy

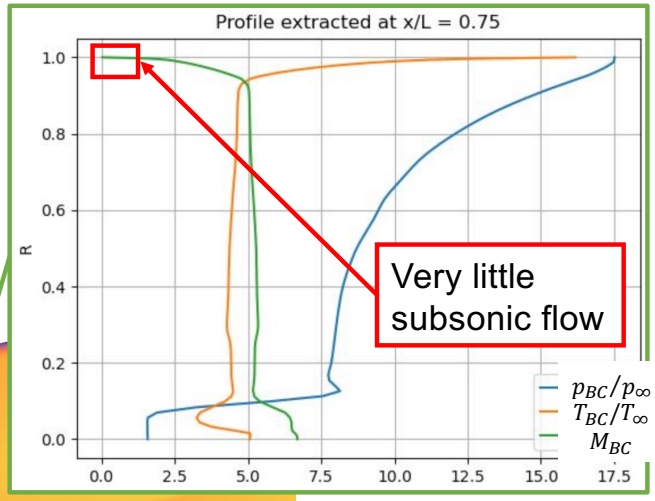
Perform unstructured steady RANS simulation of axisymmetric portion of SRP nozzle

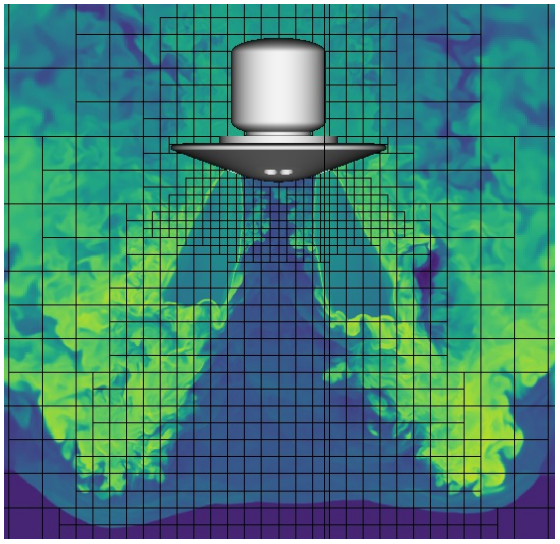
Extract RANS solution profile at supersonic location downstream of throat

Perform scale-resolving simulation of the vehicle with RANS profile as a supersonic inlet boundary condition

Steady RANS w SA model
Solution Mach Number

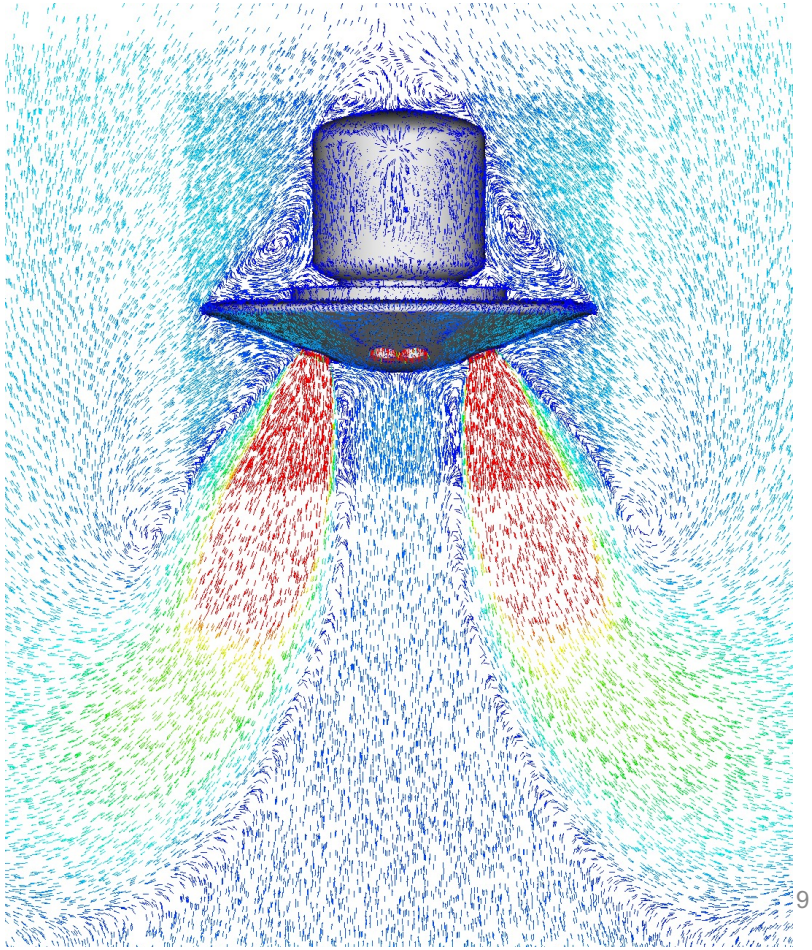






Scale-Resolving Simulation Strategy

- High-order implicit large-eddy simulation (ILES) with Cartesian AMR module
- Cartesian immersed boundary approach is appropriate because quantity of interest is integrated drag on the vehicle:
  - > 90% of axial force for unpowered vehicle is pressure drag (not viscous): Cartesian results match available RANS predictions for drag within 1%
  - Flow is massively separated on back of heat shield and on payload for both powered and unpowered vehicle
  - Flow is massively separated over large portions of heat shield due to plume entrainment and recirculation when SRP rockets are turned on



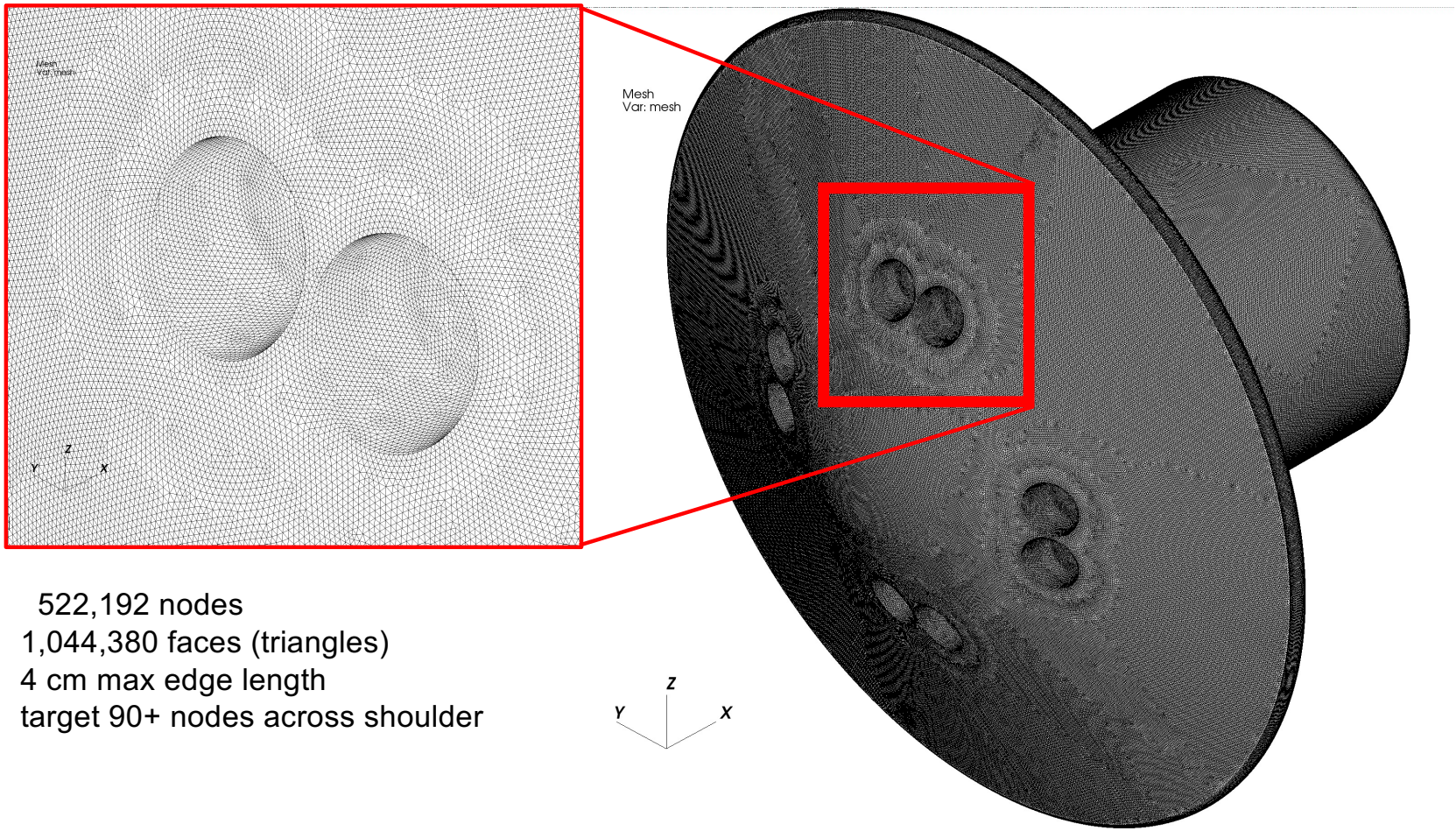
Scale-Resolving Numerical Methods



- Launch, Ascent, and Vehicle Aerodynamics (LAVA) Cartesian adaptive mesh refinement (AMR) module
  - Solves two-species Navier-Stokes (Mars atmosphere + exhaust gas)
  - Fifth-order incremental-stencil WENO shock-capturing convective flux
  - Second-order centered viscous flux
  - Second-order immersed boundary ghost-cell method
  - Explicit time integration with 3rd order Strong-Stability Preserving Runge-Kutta
  - Nozzle boundary conditions (BC) taken from precursor axisymmetric RANS simulation (radially varying supersonic outflow upstream of nozzle exit face)
  - Far-field BC: supersonic inflow/outflow, extrapolation from interior

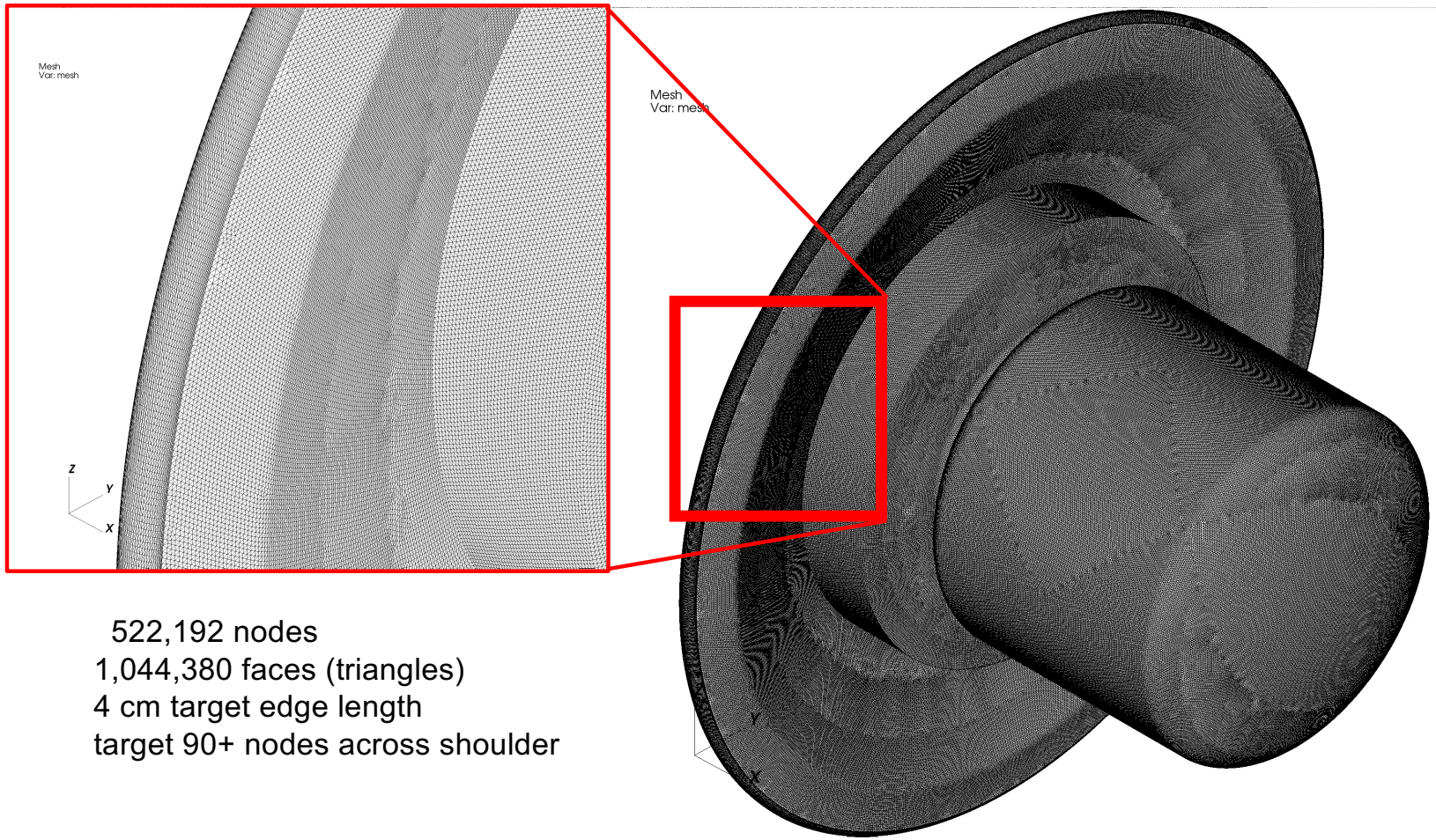
- For more details, please refer to our AIAA paper:
  - Cadieux, Francois, et al. "Scale-Resolving Simulations of Supersonic Retro-Propulsion Concept For Mars Entry, Descent, and Landing." *AIAA SCITECH 2022 Forum*. 2022.

Vehicle Surface Mesh (Front)



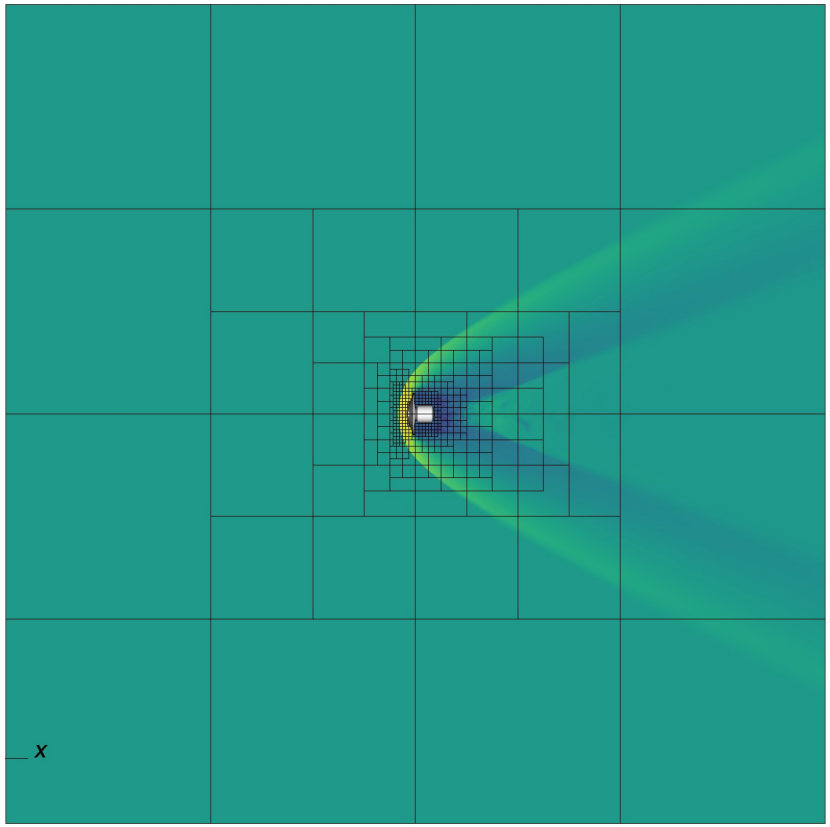
522,192 nodes
1,044,380 faces (triangles)
4 cm max edge length
target 90+ nodes across shoulder

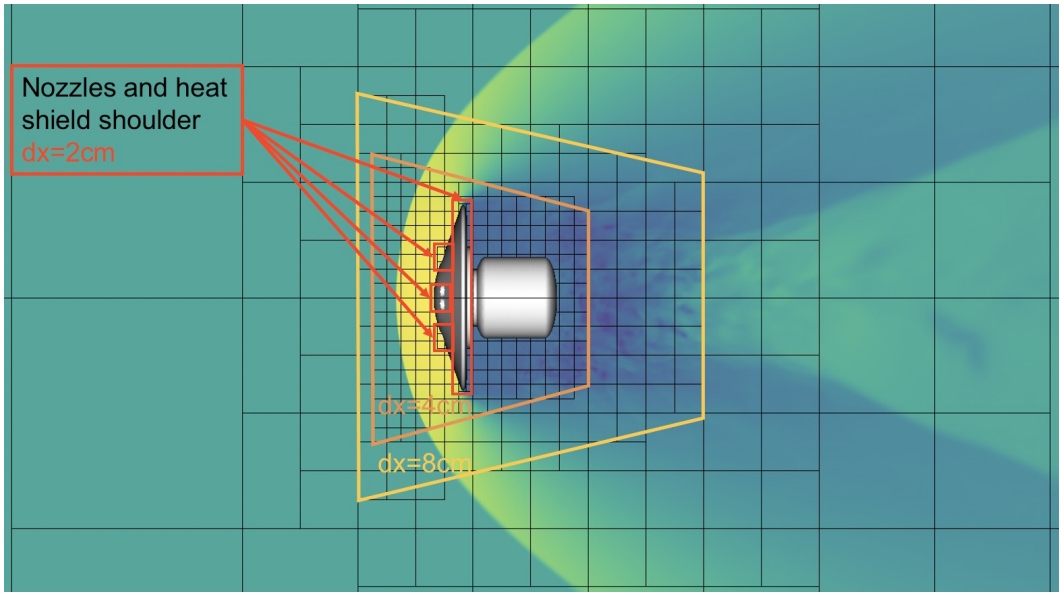
Vehicle Surface Mesh (Back)



522,192 nodes
1,044,380 faces (triangles)
4 cm target edge length
target 90+ nodes across shoulder

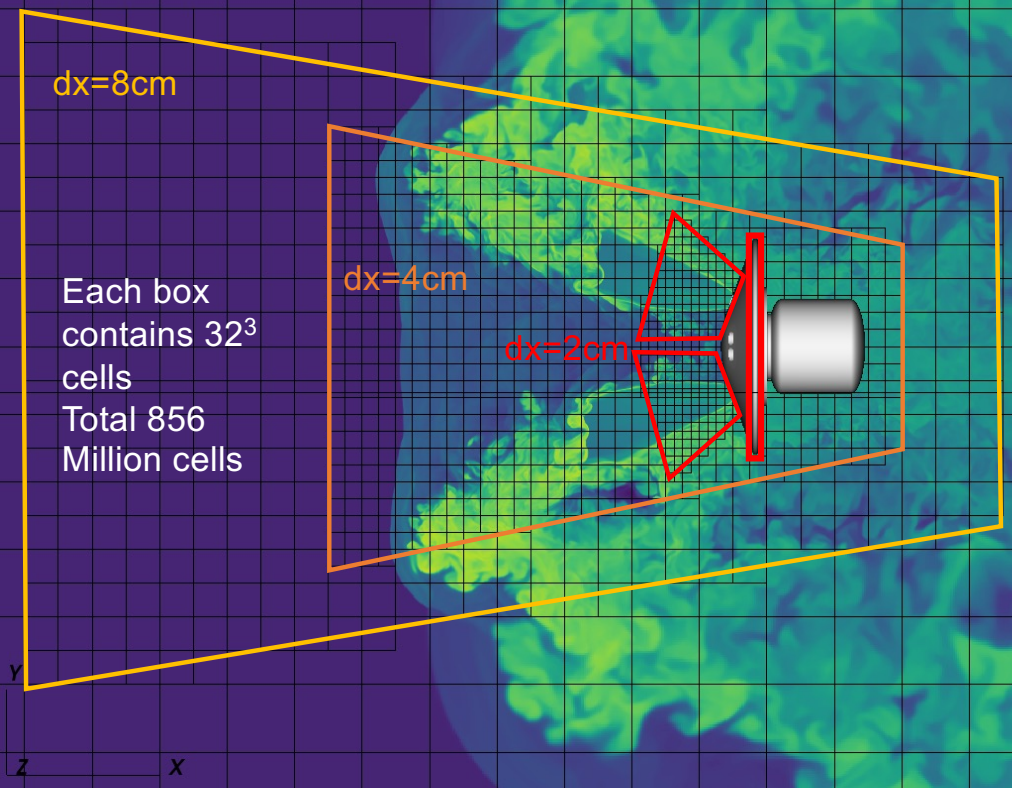
Mesh For Unpowered Simulations





Each box contains 32^3 cells. The logarithm of pressure shows the location of the bow shock and the wake structure for Mach 2.4

Mesh For Powered Simulations



Fine Mesh (856M cells)

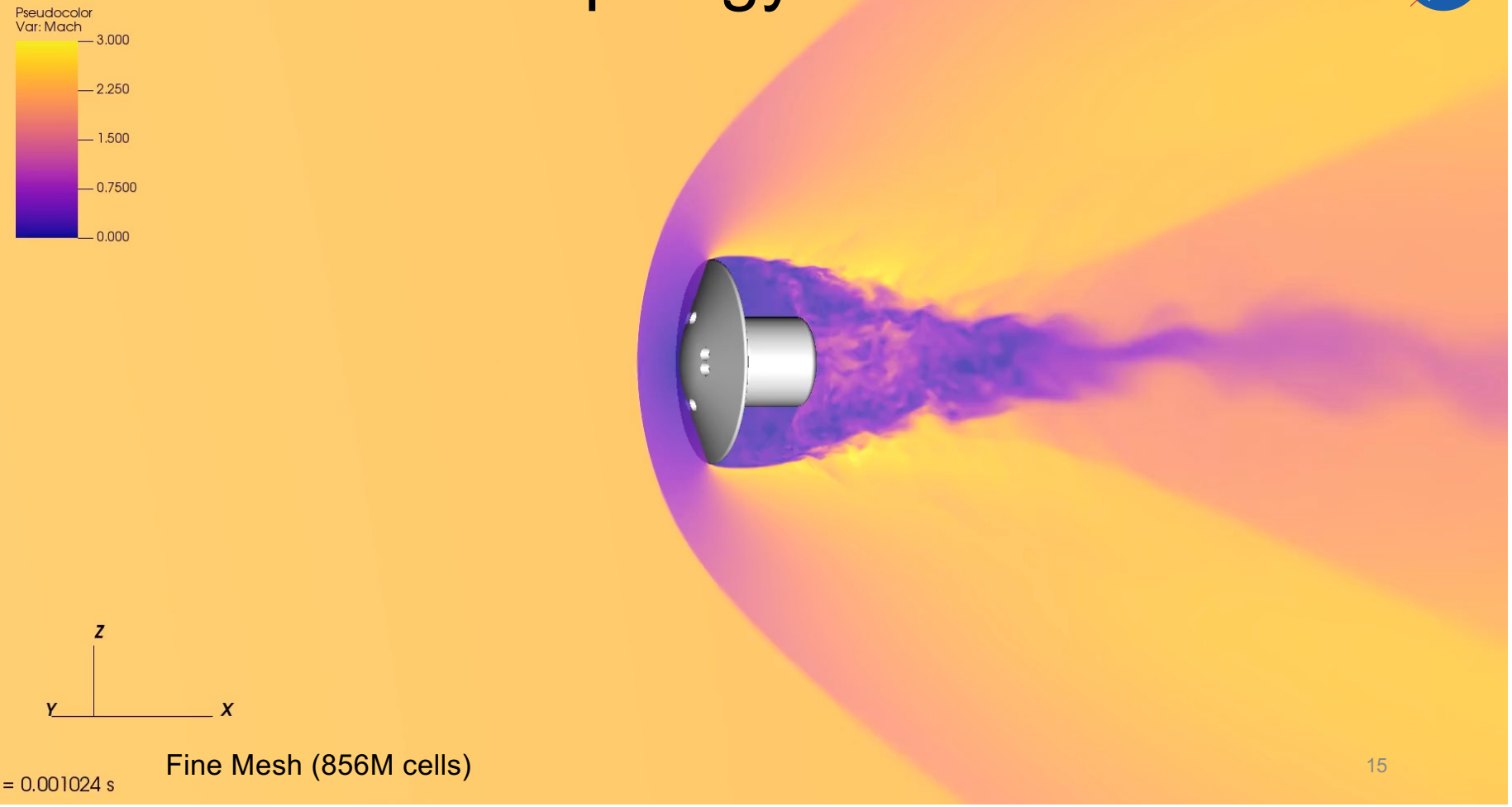
Initial conditions: Start from "converged" statistically stationary unpowered state with zero thrust, then ramp up SRP thrust linearly over 0.04 seconds

Each box contains 32^3 cells

The logarithm of temperature shows the location of the bow shock and the wake structure for Mach 2.4

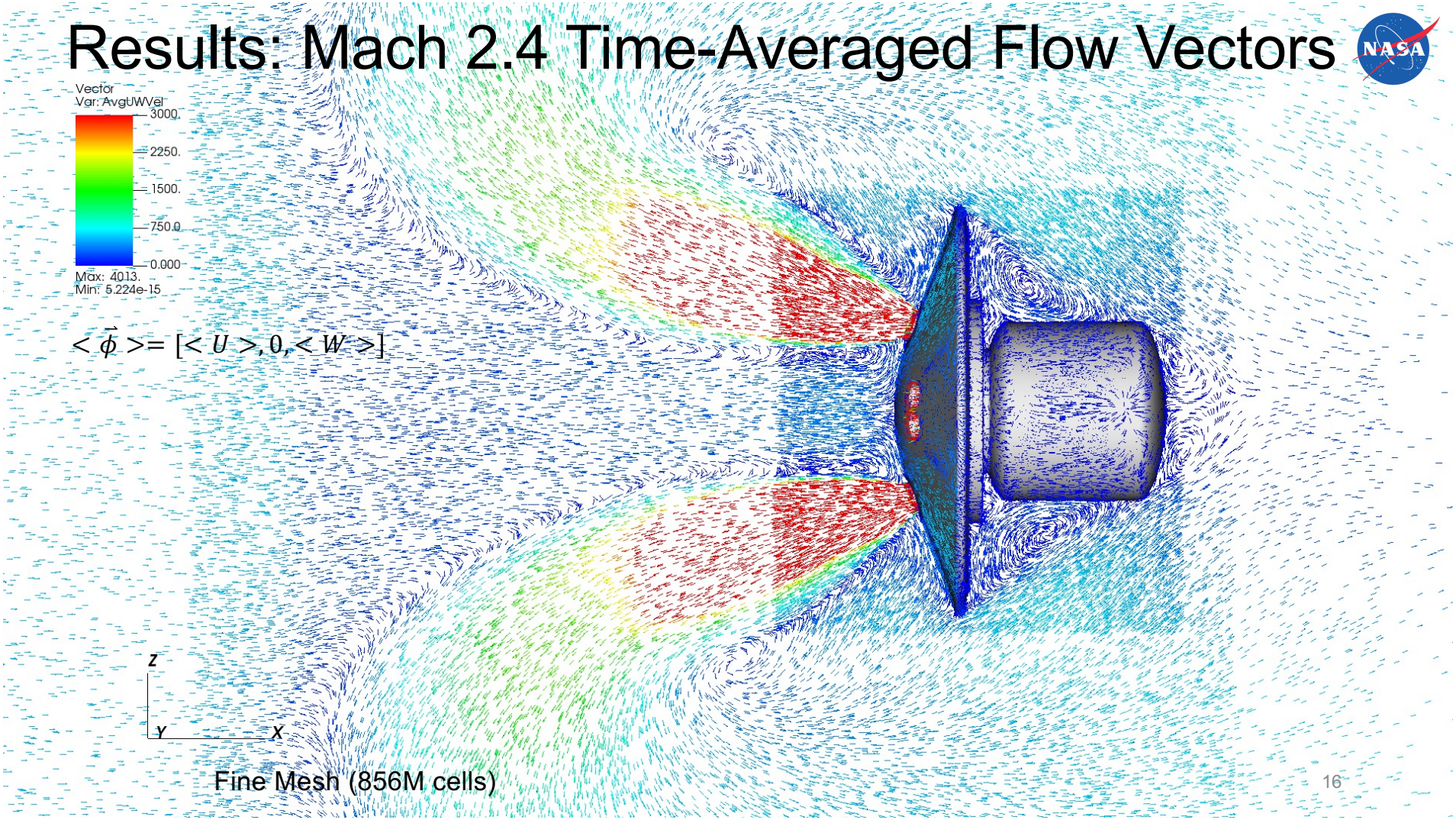
Log of temperature (blue low, yellow high) for Mach 2.4 snapshot

Results: Flow Topology at Mach 2.4



Fine Mesh (856M cells)

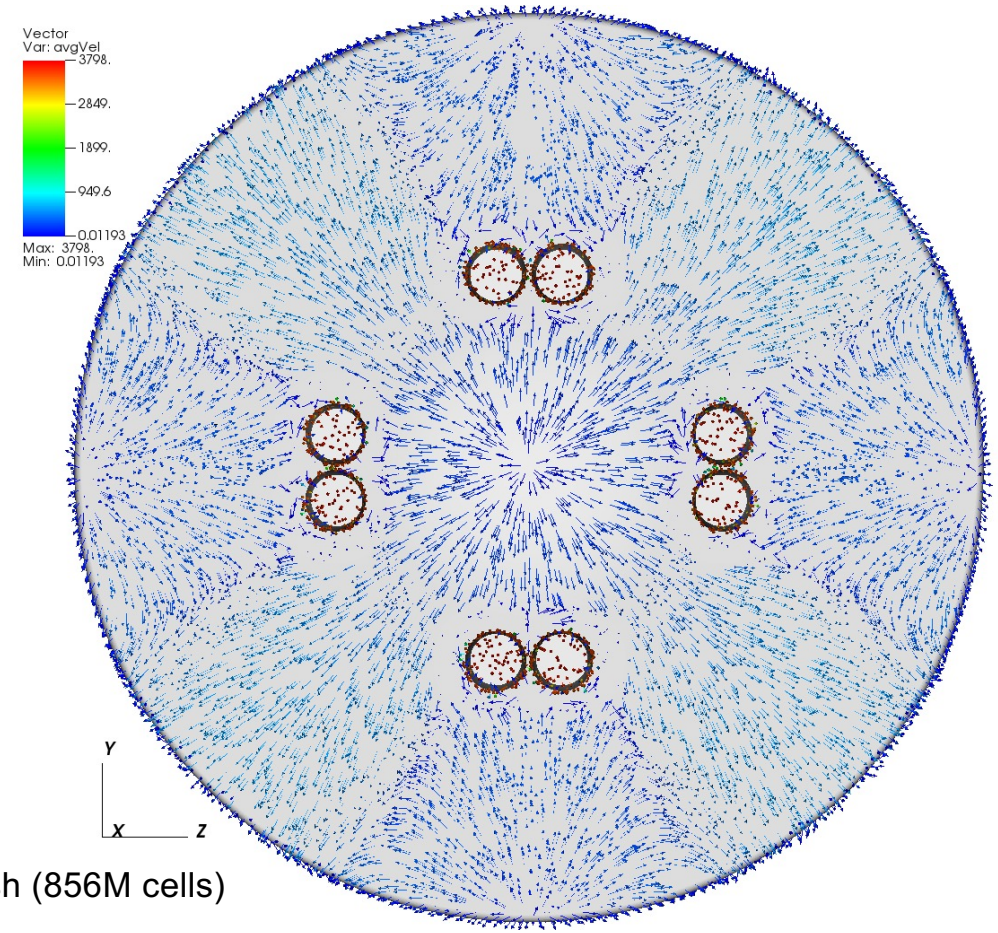
Results: Mach 2.4 Time-Averaged Flow Vectors



Fine Mesh (856M cells)

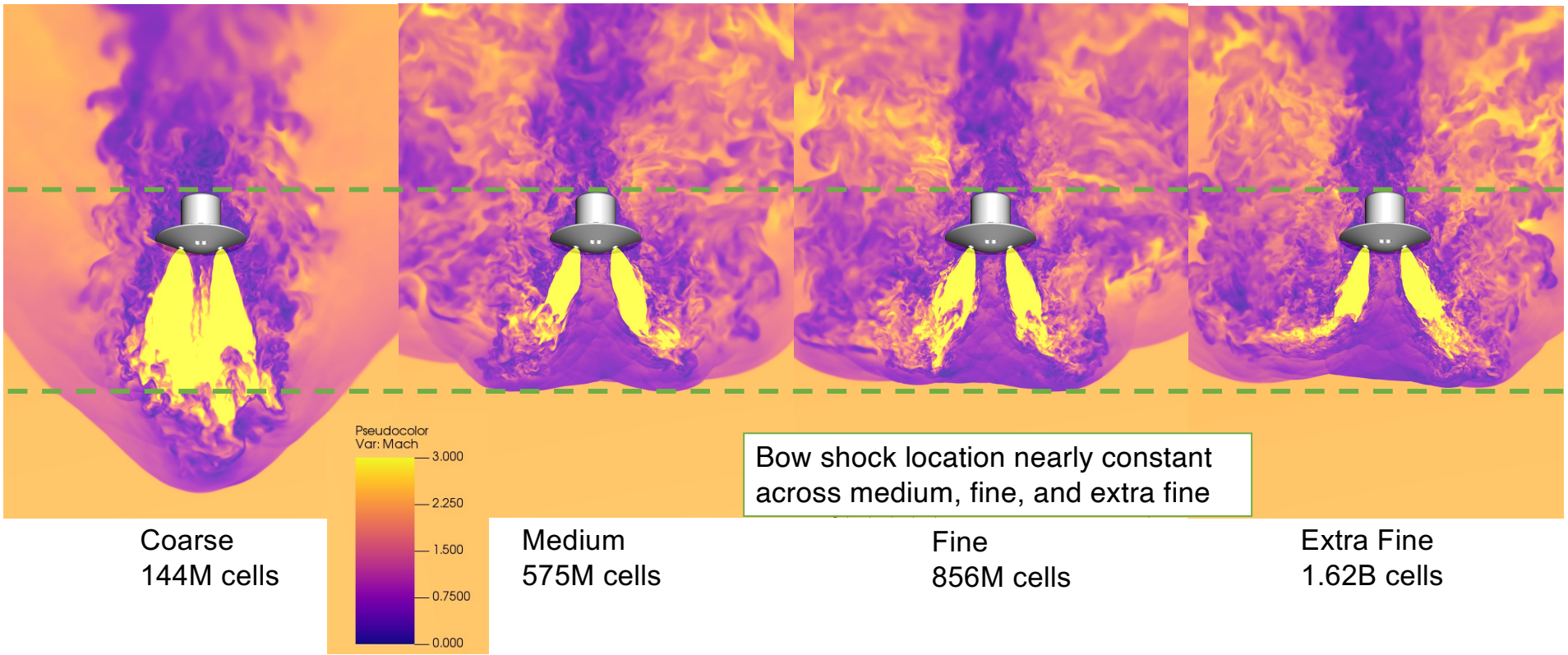
Results: Mach 2.4 Time-Averaged Flow Vectors

$< \vec{U} > - < \vec{U} > \cdot \hat{n}$



Fine Mesh (856M cells)

Results: Coarse Mesh Is Outlier (Mach 2.4)



Coarse
144M cells

Medium
575M cells

Fine
856M cells

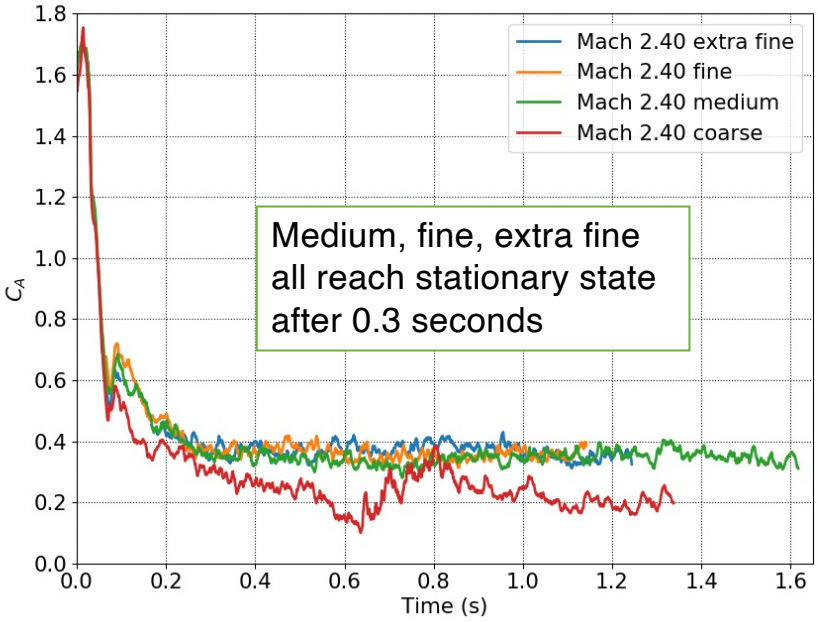
Extra Fine
1.62B cells

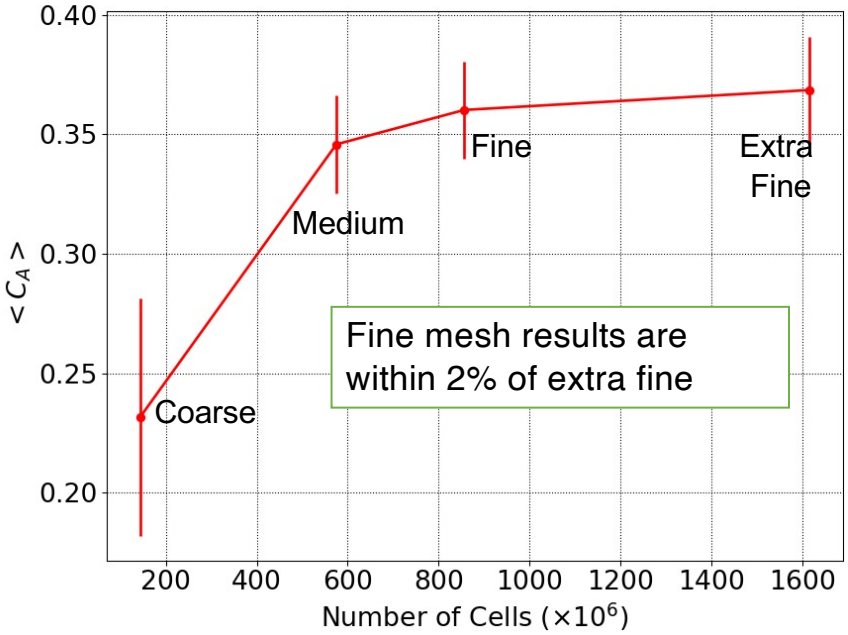
Results: Detailed Flow Viz at 1.6B Cells



Extra Fine mesh (1.6B cells) simulation showing temperature on a cut plane through the center-left nozzles and on the vehicle surface where yellow is high and purple is low. *Video Credit: Timothy Sandstrom*

Results: Grid Convergence Study

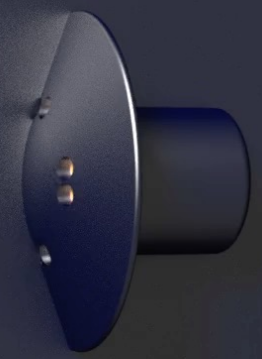




Convergence across medium, fine and extra fine meshes

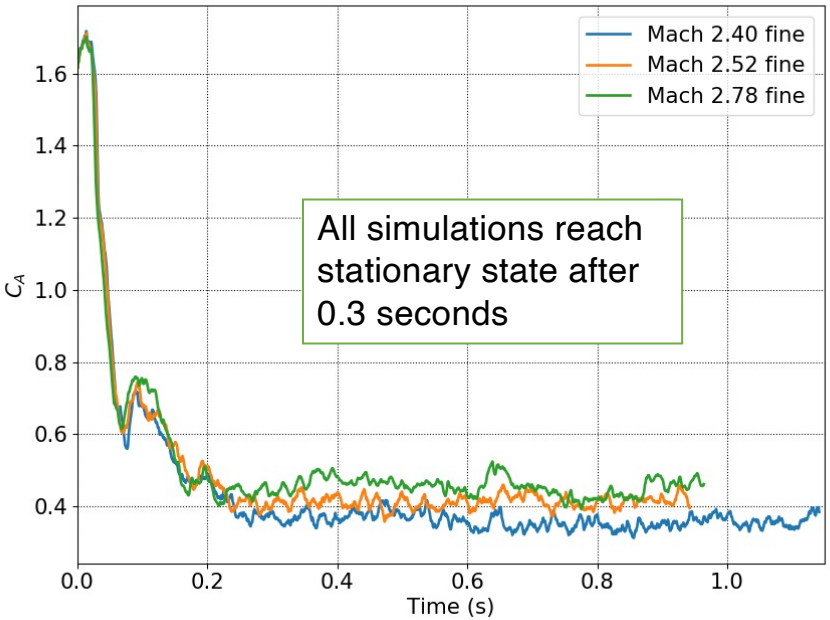
Apparent Order (p)	Grid Convergence Index	Estimated Converged $< C_A >$	Estimated Uncertainty in $< C_A >$
2.336	0.039	0.368	±0.014

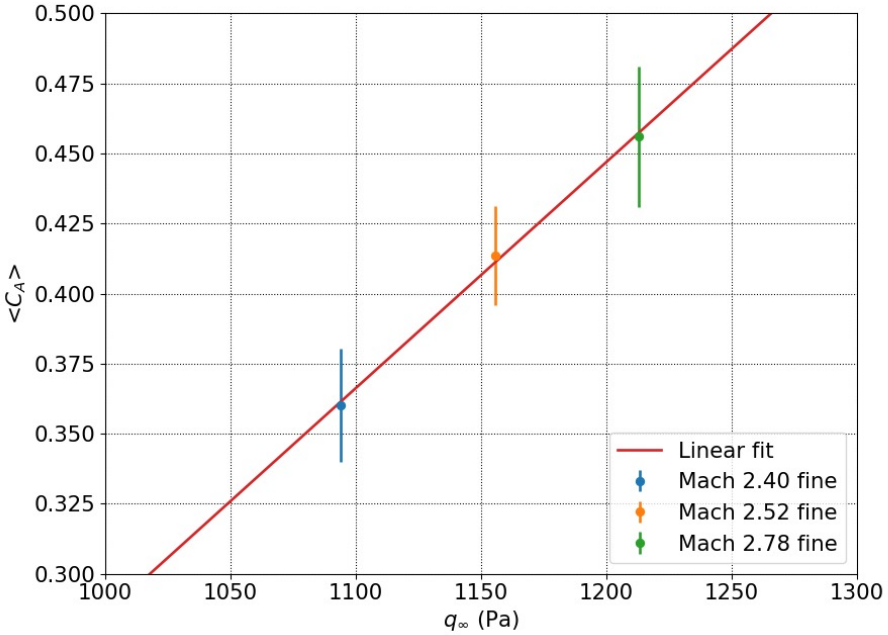
Results: Flow Topology At Mach 2.52



Fine mesh (856M cells) simulation showing exhaust mass fraction on a cut plane through the center-left nozzles and on the vehicle surface where white is 100% and black is 1%.
Video Credit: Timothy Sandstrom

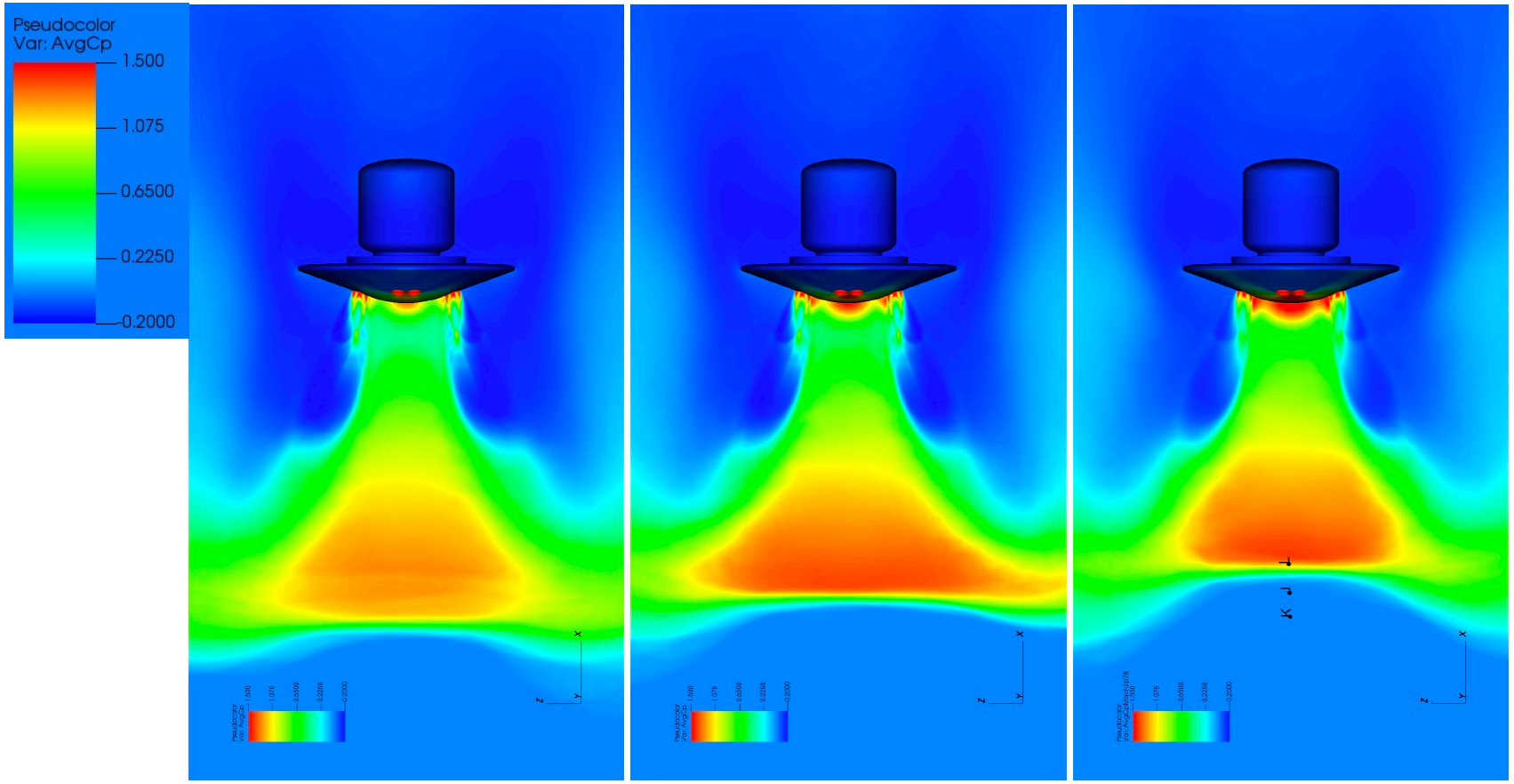
Results: Altitude and Mach Number Trends





Motor thrust is fixed to 80 kN. As incoming dynamic pressure (q_∞) increases, it pushes bow shock closer to vehicle and increases pressure recovery on heat shield and thus $< C_A >$ increases. More details are available in full paper.

Results: Time-Averaged Pressure Coefficient



(a) Mach 2.4 (b) Mach 2.52 (c) Mach 2.78

Computational Resources



For 1 second of time integration

Case	Cell Count ($\times 10^6$)	Node Type	Core Count	Wall Time (Days)	Core-Hours	NASA SBU
Unpowered Fine	188	Intel Broadwell	2,800	0.500	33,600	1,200
Powered Medium	575	Intel Broadwell	6,020	4.375	632,100	22,575
Powered Fine	856	Intel Broadwell	6,020	7.368	1,064,500	38,019
Powered Extra Fine	1,615	AMD Rome	12,800	7.610	2,337,800	74,152

- Precursor nozzle RANS simulations are meshed and completed in ~2 hours on 1 linux workstation
- All scale-resolving simulations were completed within ~5 weeks time frame
- Powered simulations were run in approx. 1 week with priority
- Without priority, a typical powered simulation would take 2 to 3 weeks due to wait-time

Optimizing For Shorter Turnaround Time



For 1 second of powered time integration

Case	Cell Count ($\times 10^6$)	Node Type	Core Count	Wall Time (Days)	Core-Hours	NASA SBU
Medium	575	Broadwell	6,020	4.375	632,100	22,575
Optimized Medium*	300	Skylake	4,000	0.913	87,680	3,484
				4x faster turnaround		6x fewer resources

Computer Science Improvements

- Non-blocking overlapped communication
- Improved load balance
- Optimized kernels and inter-level operators
- Composite time integration (instead of subcycled) for higher accuracy and CFL-based time integration
- Buffered surface output and improved parallel volume output

CFD Improvements

- Trimmed mesh "fat" by moving from 32^3 to 8^3 refinement boxes (identical refinement regions)
- Quicker mesh coarsening outside of maximum bow shock standoff distance (x ~ -32m)
- Reduced plume refinement regions radius (flared cylinders) at their wide end (~5 meters away from nozzle exit) from 5.4 to 4.4 meters

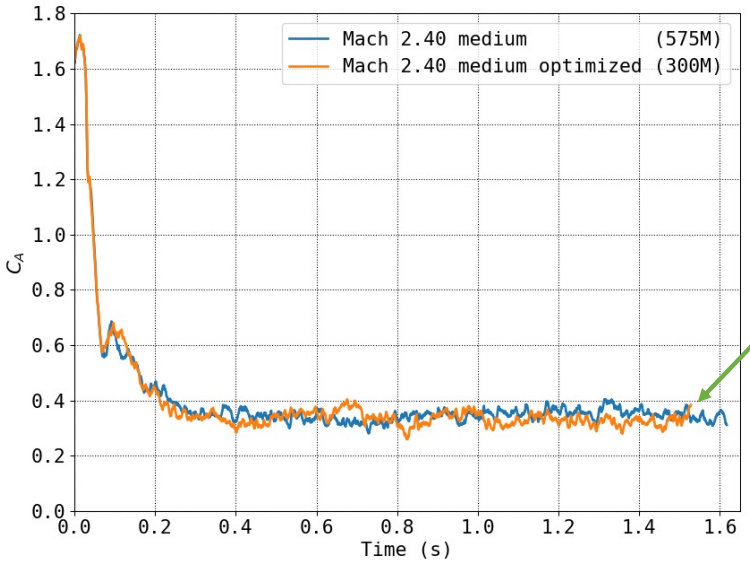
Accuracy Is Maintained

For 1 second of powered time integration

Case	Cell Count ($\times 10^6$)	Node Type	Core Count	Wall Time (Days)	Core-Hours	NASA SBU
Medium	575	Broadwell	6,020	4.375	632,100	22,575
Optimized Medium*	300	Skylake	4,000	0.913	87,680	3,484

4x faster turnaround

6x fewer resources



Predicts time-averaged axial force coefficient within 3.6% from previous simulation

Summary



- Performed scale-resolving simulations of a conceptual Mars EDL vehicle at three Mach numbers corresponding to altitudes where the plumes are over-expanded with the Launch, Ascent, and Vehicle Aerodynamics (LAVA) Cartesian AMR module

- Obtained excellent grid convergence in time-average axial force coefficient for Mach 2.4 and showed that the estimated grid-related uncertainty is smaller than the unsteady standard deviation

- Demonstrated that scale-resolving simulations of SRP for a few trajectory points can be completed within reasonable turnaround time on current NASA HECC resources (regular queues) and could be utilized to support future engineering decisions

Forward Looking Development Efforts



- Wall-modeled LES: currently underway, with impressive results for high-lift prediction workshop
- Free flight capability: tackle deceleration (3 and 6 DOF), currently underway for supersonic parachute fluid-structure interaction (FSI) capability
- Code performance optimization: currently underway for CPU, exploring GPU as well
- Participate in further validation studies as opportunities arise

Acknowledgements



Mach 2.4 Fine Mesh (856M cells): Volume rendering of exhaust mass fraction where yellow is 100% and black is 1%. Only the plumes on the left side of vehicle are rendered to elucidate the plume structure without obstruction. *Video credit: Timothy Sandstrom*

- Ashley Korzun for providing the vehicle geometry and motor exhaust gas thermodynamic properties
- Computer resources provided by NASA Advanced Supercomputing (NAS) Facility
- Timothy Sandstrom and NAS visualization team for some of the animations
- James Jensen and Elisha Makarevich for preparing the surface mesh and the cut planes
- Jeff Housman and Emre Sozer for their insights and guidance